INSTITUTE OF PHYSICS PUBLISHING PHYSICAL BIOLOGY
Phys. Biol. **1** (2004) 229–235 PII: S1478-3967(04)82412-4

Min-protein oscillations in round bacteria

Kerwyn Casey Huang[1,2,3] **and Ned S Wingreen**[2,3]

[1] Department of Physics, Massachusetts Institute of Technology, 77 Massachusetts Avenue, Cambridge, MA 02139, USA
[2] NEC Laboratories America, Inc., 4 Independence Way, Princeton, NJ 08540, USA

E-mail: kchuang@princeton.edu and wingreen@princeton.edu

Received 23 June 2004
Accepted for publication 25 November 2004
Published 31 December 2004
Online at stacks.iop.org/PhysBio/1/229
doi:10.1088/1478-3967/1/4/005

Abstract
In rod-shaped *Escherichia coli* cells, the Min proteins, which are involved in division-site selection, oscillate from pole-to-pole. The homologs of the Min proteins from the round bacterium *Neisseria gonorrhoeae* also form a spatial oscillator when expressed in wild-type and round, *rodA*$^-$ mutants of *E. coli*, suggesting that the Min proteins form an oscillator in *N. gonorrhoeae*. Here we report that a numerical model for Min-protein oscillations in rod-shaped cells also produces oscillations in round cells (cocci). Our numerical results explain why the MinE-protein rings found in wild-type *E. coli* are absent in round mutants. In addition, we find that for round cells there is a minimum radius below which oscillations do not occur, and a maximum radius above which oscillations become mislocalized. Finally, we demonstrate that Min-protein oscillations can select the long axis in nearly round cells based *solely* on geometry, a potentially important factor in division-plane selection in cocci.

Introduction

In the rod-shaped bacterium *Escherichia coli*, the proteins MinC, MinD and MinE are observed to oscillate from pole to pole [1–4] every ∼20 s [2]. Both MinD and MinE are required for oscillations [2]; MinC is not required, but is observed to oscillate because it forms complexes with MinD on the membrane [5]. MinD is an ATPase which associates to the membrane and forms helical polymers there [6] in its ATP-bound form (MinD:ATP) [7]. MinE is recruited to the membrane by MinD, where it activates hydrolysis of MinD:ATP resulting in dissociation of MinD from the membrane [7]. The oscillations concentrate MinCD complexes near the poles of the cell, where MinC blocks formation of a ring of FtsZ protein [8]. Formation of this FtsZ ring is required to initiate septum formation and cell division [9], so the net effect of the Min oscillations is to block cell divisions near the poles (minicelling). Placement of the FtsZ ring is also regulated by nucleoid occlusion [10–12], a mechanism which blocks FtsZ ring formation in the vicinity of a nucleoid.

Homologs of the Min proteins have also been identified in round cells. In the coccus *Neisseria gonorrhoeae*, loss of $MinD_{Ng}$ results in abnormal cell division and morphology, and decreased cell viability [13]. $MinD_{Ng}$ and $MinE_{Ng}$ from *N. gonorrhoeae* were observed to oscillate when expressed in *E. coli* lacking its own MinD and MinE [14]. To date, there has been no direct observation of Min-protein oscillations in *N. gonorrhoeae* because of resolution limits associated with the small size of the bacteria, typically around 0.5 μm in radius [13]. However, in round *E. coli* cells, resulting from disruption of the *rodA* gene, both native MinD [15] and $MinD_{Ng}$ from *N. gonorrhoeae* [14] have been observed to oscillate. Interestingly, while oscillations in wild-type *E. coli* display a ring of MinE protein, no MinE ring is observed in the round *rodA*$^-$ cells. Taken together, the close homology of the *E. coli* and *N. gonorrhoeae* Min proteins, the complementation experiments and the Min oscillations in round *E. coli* cells suggest that the Min proteins also form an oscillator in *N. gonorrhoeae* [14].

Here we demonstrate that a numerical model for Min-protein oscillations in rod-shaped cells [17] also leads to oscillations in round cells. The model is shown schematically in figure 1, and involves only *in vitro* observed interactions of MinD and MinE [2, 7]. In contrast to earlier modeling attempts [18–20], the model in [17] is fully three-dimensional,

[3] Present address: Department of Molecular Biology, Princeton University, Princeton, NJ 08544, USA.

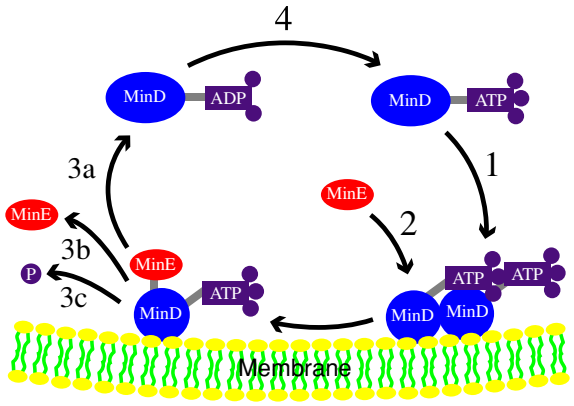

Figure 1. Model MinD,E cycle driven by ATP hydrolysis. (1) Cytoplasmic MinD:ATP complex attaches to the membrane, preferentially where other MinD:ATP is bound. (2) MinE in the cytoplasm attaches to a membrane-associated MinD:ATP complex. (3) MinE activates ATP hydrolysis by MinD, breaking apart the complex, and releasing (*a*) MinD:ADP, (*b*) MinE and (*c*) phosphate into the cytoplasm. (4) MinD:ADP is converted back to MinD:ATP by nucleotide exchange. In wild-type cells, MinE is likely active as a homodimer [16].

so that extension to round cells is straightforward. The oscillations are driven by a cycle in which MinD:ATP binds to the membrane, preferentially at locations of high pre-existing concentrations of MinD:ATP. MinE then attaches to the membrane-bound MinD:ATP, activates ATP hydrolysis and MinE and MinD:ADP reenter the cytoplasm. In the cytoplasm, MinD:ADP undergoes nucleotide exchange to MinD:ATP to become competent to rebind the membrane.

Reaction–diffusion equations

The equations describing the time evolution of MinD and MinE concentrations in a spherical cell of radius R (see schematic of reaction cycle in figure 1) are

$$\frac{\partial \rho_{D:\mathrm{ADP}}}{\partial t} = \mathcal{D}_D \nabla^2 \rho_{D:\mathrm{ADP}} - \sigma_D^{\mathrm{ADP}\to\mathrm{ATP}} \rho_{D:\mathrm{ADP}} + \delta(r-R)\sigma_{de}\rho_{de} \tag{1}$$

$$\frac{\partial \rho_{D:\mathrm{ATP}}}{\partial t} = \mathcal{D}_D \nabla^2 \rho_{D:\mathrm{ATP}} + \sigma_D^{\mathrm{ADP}\to\mathrm{ATP}} \rho_{D:\mathrm{ADP}} - \delta(r-R) \times [\sigma_D + \sigma_{dD}(\rho_d + \rho_{de})] \left(\frac{\rho_{\max} - \rho_d - \rho_{de}}{\rho_{\max}} \right) \rho_{D:\mathrm{ATP}} \tag{2}$$

$$\frac{\partial \rho_E}{\partial t} = \mathcal{D}_E \nabla^2 \rho_E + \delta(r-R)\sigma_{de}\rho_{de} - \delta(r-R)\sigma_E \rho_d \rho_E \tag{3}$$

$$\frac{\partial \rho_d}{\partial t} = -\sigma_E \rho_d \rho_E(R) + [\sigma_D + \sigma_{dD}(\rho_d + \rho_{de})] \times \left(\frac{\rho_{\max} - \rho_d - \rho_{de}}{\rho_{\max}} \right) \rho_{D:\mathrm{ATP}}(R) \tag{4}$$

$$\frac{\partial \rho_{de}}{\partial t} = -\sigma_{de}\rho_{de} + \sigma_E \rho_d \rho_E(R) \tag{5}$$

where $\rho_{D:\mathrm{ADP}}$, $\rho_{D:\mathrm{ATP}}$, ρ_E are the concentrations in the cytoplasm of MinD:ADP complexes, MinD:ATP complexes, and MinE and ρ_d, ρ_{de} are the concentrations on the membrane of MinD:ATP and MinD:MinE:ATP complexes. Simulations with an intermediate free MinD species in the cytoplasm, thereby converting the single rate constant $\sigma_D^{\mathrm{ADP}\to\mathrm{ATP}}$ into two separate decay rates, do not show any significant differences.

The delta functions, $\delta(r-R)$, represent local exchange of proteins between membrane and cytoplasm. The total concentrations of MinD and MinE are 1275 $\mu\mathrm{m}^{-3}$ and 450 $\mu\mathrm{m}^{-3}$, respectively (assuming MinE is active as a homodimer, this implies 900 MinE monomers $\mu\mathrm{m}^{-3}$) [21]. The diffusion constants are

$$\mathcal{D}_D = \mathcal{D}_E = 2.5\ \mu\mathrm{m}^2\,\mathrm{s}^{-1},$$

as measured for the cytoplasmic diffusion of a maltose binding protein in the *E. coli* cytoplasm [22], and the reaction rates are

$$\sigma_D^{\mathrm{ADP}\to\mathrm{ATP}} = 1\,\mathrm{s}^{-1}, \qquad \sigma_D = 0.025\,\mu\mathrm{m\,s}^{-1},$$
$$\sigma_{dD} = 0.0015\,\mu\mathrm{m}^{-3}\,\mathrm{s}^{-1}, \qquad \sigma_{de} = 0.4\,\mathrm{s}^{-1},$$
$$\sigma_E = 0.3\,\mu\mathrm{m}^{-3}\,\mathrm{s}^{-1}.$$

The factor $(\rho_{\max} - \rho_d - \rho_{de})/\rho_{\max}$ in equations (2) and (4) prevents overcrowding on the membrane. The maximum allowed density is $\rho_{\max} = 2000\ \mu\mathrm{m}^{-2}$. We have modified the MinE binding and hydrolysis rates from [17] to induce oscillations in round cells of radius $R \sim 0.5\ \mu$m or larger. While there is no reason *per se* that the binding and hydrolysis rates would necessarily be identical for *N. gonorrhoeae* and *E. coli* proteins, we have verified that these new parameters also produce oscillations with a period of 80 s in rod-shaped cells of length 4 μm and radius 0.5 μm that are qualitatively identical to those in our previous work [17]. We discretized and solved equations (1)–(5) on a three-dimensional lattice in spherical coordinates, with grid spacing $\mathrm{d}r = 0.05\ \mu$m, $\mathrm{d}\theta = \mathrm{d}\phi = \pi/20$.

Results and discussion

Min-protein oscillations with no MinE ring

The results of numerical integration in time of the model equations (cf figure 1 and equations (1)–(5)) for a spherical cell with radius $R = 0.5\ \mu$m are shown in figure 2. In the spherical cell, any initial protein distributions (except those with perfect spherical symmetry) generate an oscillation which is rotationally symmetric about a 'north–south' axis. The choice of oscillation axis does depend on initial conditions; in figure 2 we have restricted the initial concentrations to be uniform in the azimuthal direction. The oscillation cycle has a period of 81 s. As in cylindrical cells [17], zones of MinD:ATP grow from and shrink to the poles of the cell. However, in contrast to cylindrical cells, there is a notable absence of a MinE ring; rather, the MinE spreads throughout the entire MinD:ATP polar zone. The bottom row of panels in figure 2 shows the quantities in columns (*a*–*c*) averaged over one complete oscillation. The minimum for membrane-bound MinD:ATP occurs at the equator, indicating the most likely division site due to lower concentrations of the FtsZ ring-inhibitor MinC.

Periodic oscillations occur for a wide range of model parameters. The period can be increased without limit by reducing the hydrolysis rate σ_{de}. Increasing σ_{de} reduces the

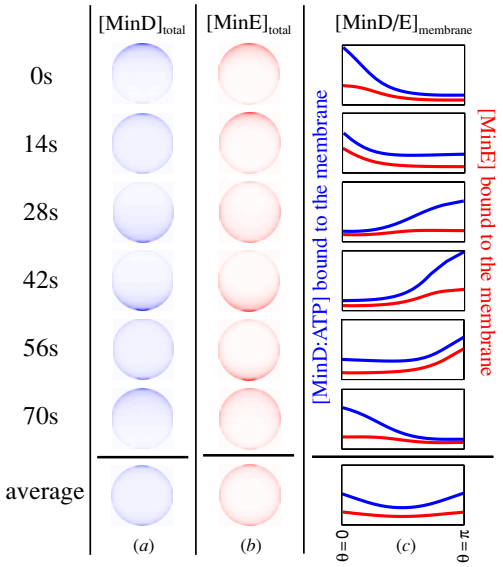

Figure 2. Time slices in 14 s increments of one complete MinD,E oscillation in a spherical cell with radius $R = 0.5\ \mu$m. To mimic experimental observations of GFP fluorescence, we show two-dimensional projections onto the x–z plane (where the solution is rotationally symmetric about the z-axis) of the concentrations of (*a*) MinD and (*b*) MinE. In (*a*), the MinD polar zone shrinks toward the south pole, and reforms at the north pole. In (*b*), the MinE also forms a polar zone which lags behind the MinD distribution. Note the absence of a MinE ring. Except during brief cytoplasmic-burst phases (14 s, 56 s for MinD) both MinD and MinE are primarily membrane bound. (*c*) shows the membrane-associated concentrations as a function of polar angle θ, MinD:ATP in blue and MinE in red. The y-axis on each plot ranges from 0 to 500 μm^{-2}.

period down to a minimum of 70 s, beyond which point most of the MinD is cytoplasmic and there are no oscillations. Oscillations also occur for a range of protein concentrations, with the period proportional to the ratio $[\mathrm{MinD}]/(\sigma_{de}[\mathrm{MinE}])$ [17], reflecting the time required for MinE to hydrolyze a MinD:ATP polar zone.

The basic mechanism for these oscillations is that a typical MinD, once released from the membrane, diffuses farther in the cytoplasm than a typical MinE before reattaching to the membrane. This allows formation of a new zone of MinD:ATP at the opposite pole, while MinE is at work progressively hydrolyzing the old polar zone. Growth of the new polar zone mirrors a gradient of MinD:ATP in the cytoplasm caused by the stickiness of the old polar zone [17]. The delay for nucleotide exchange allows MinD:ADP to diffuse away from the old polar zone and is essential to establishment of the cytoplasmic gradient. The absence of a visible MinE ring in our simulations (figure 2) can be understood as purely an effect of geometry, as shown in figures 3(*a*) and (*b*). In either a round or a rod-shaped cell, a MinE that escapes the MinD:ATP zone at one pole of the cell is likely to rebind where it first contacts the opposite polar zone. In a round cell, the likelihood of first contact is roughly equal everywhere in the new polar zone as shown in figure 3(*a*). In a rod-shaped cell, however, the first contact is likely to occur near the medial edge of the new polar zone, attenuating the probability for first contact farther toward the pole, and resulting in a MinE ring as shown in figure 3(*b*).

To test this geometrical model, we performed simulations with MinE proteins released from one pole in both cylindrical and spherical geometries. The MinE proteins start diffusing from the center of one end of the cylinder and the north pole of the sphere. For a cylinder with radius 0.5 μm and length 4 μm, we approximate the new polar zone by a region of constant binding on the opposite half cylinder ($z \in [2, 4]\ \mu$m) with rate $\sigma = 0.5\ \mu\mathrm{m\ s}^{-1}$. For a sphere with radius 0.5 μm, we approximate the new polar zone as the southern hemisphere with the same constant binding rate σ. Two-dimensional projected images of the final membrane concentrations of MinE are shown in figures 3(*c*) and (*d*), with the densities shown in figures 3(*e*) and (*f*). In the sphere the MinE density is nearly uniform throughout the southern hemisphere, while in the cylinder the MinE density shows a clear central peak, i.e., a MinE ring.

Oscillations in nearly round cells

Real cells are not perfectly round. In nearly round *rodA*$^-$ mutants of *E. coli*, Min-protein oscillations were almost always observed to orient along the long axis [15]. While this orientation could be due to membrane targets or scars, we ask whether the geometry of the cell alone could be sufficient to orient the Min oscillations. In figure 4, we show the results of numerical integration in time of equations (1)–(5) for an ellipsoidal cell with semi-major axis of length $R_1 = 0.525\ \mu$m and semi-minor axes of length $R_2 = 0.5\ \mu$m, starting from a *completely random* distribution of proteins. All diffusion constants, rate constants and mean volume concentrations are the same as for the spherical cell in figure 2. Within a few oscillation periods, a stable oscillation is established precisely along the long axis of the ellipsoidal cell with a period of 80 s.

Minimum radius for oscillations

We find that spherical cells below a minimum radius $R_{\min}$ do not support oscillations. The exact value of $R_{\min}$ depends on the choice of parameters; for our choice $R_{\min} = 0.45\ \mu$m. The non-oscillating solution of equations (1)–(5) is spherically symmetric and has uniform concentrations of MinE and total MinD in the cytoplasm, which lacks sources or sinks of these proteins. However, the concentrations of the two species MinD:ADP and MinD:ATP can individually vary in the radial direction due to local exchange with the membrane. To analyze stability, we solve for the static concentrations: $\rho_i^0(r)$ where $i \in \mathcal{S} = \{D\text{: ADP}, D\text{: ATP}, E, d, de\}$, and then perturb about this static solution:

$$\rho_i^0(r) \to \rho_i^0(r)[1 + \varepsilon P_l(\cos\theta)], \tag{6}$$

where P_l is the lth Legendre polynomial, which is an eigenmode of the angular part of the diffusion equation in spherical coordinates with eigenvalue $\nu_l = l(l+1)/r^2$. In

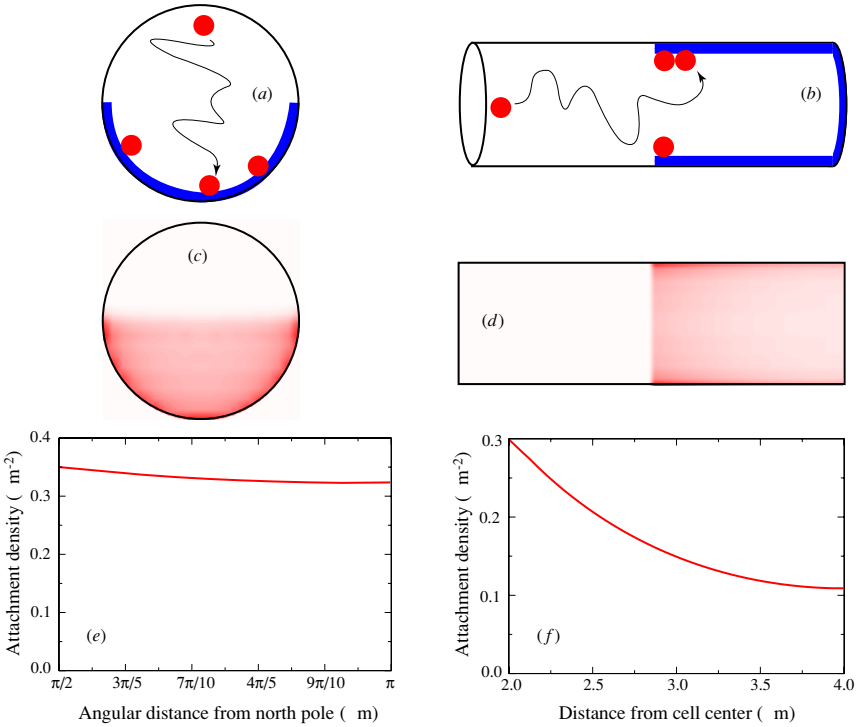

Figure 3. Geometric explanation for the absence of a MinE ring in round cells. (*a*) A MinE released from one pole of a round cell is approximately equally likely to bind anywhere within the new MinD zone at the opposite pole. (*b*) A MinE released from one pole of a rod-shaped cell is more likely to contact and bind to the nearest part of the new MinD polar zone. In rod-shaped cells, the result is a MinE 'ring'—an accumulation of MinE near the medial edge of the new polar zone. (*c*), (*d*) Projected images of MinE attachment densities and (*e*), (*f*) quantified attachment densities (normalized to 1 MinE molecule) for MinE release and attachment simulations described in the text.

practice, we define the cytoplasmic densities on a grid of size $n_r = R/\mathrm{d}r$:

$$\rho_i^0(r) \to \left(\rho_i^0\right)_j\Big|_{j=1}^{n_r}. \tag{7}$$

The perturbations in equation (6) evolve in time according to

$$\rho_i = \rho_i^0(r)[1 + \varepsilon\, \mathrm{e}^{\Lambda t} P_l(\cos\theta)], \tag{8}$$

where the exponent $\Lambda \equiv \Lambda_1 + \mathrm{i}\Lambda_2$, is an eigenvalue of the matrix $\mathbf{H} - \nu_l\mathbf{D}$. The Hessian matrix $\mathbf{H}$ is

$$\mathbf{H} = \left[\frac{\partial\left(\rho_i^0\right)_j}{\partial\left(\rho_k^0\right)_m}\right], \tag{9}$$

where i, k run over species in $\mathcal{S}$ and $j, m = 1$ if $i, k \in \{d, e\}$ and $j, m = 1, \ldots, n_r$ otherwise. The diffusion matrix is

$$\mathbf{D} = [D_{ij}], \tag{10}$$

where $D_{ij} \equiv \delta_{ij}\mathcal{D}_i$ and $\mathcal{D}_i$ is the diffusion constant of species ρ_i. Any mode with instability exponent $\Lambda_1 > 0$ represents an unstable (growing) perturbation about the static solution, and indicates that the solution of equations (1)–(5) is oscillatory.

In figure 5(*a*), we plot the period of full nonlinear oscillations and in figure 5(*b*) the growth-rate exponent Λ_1 for the most unstable perturbation ($\sim\cos\theta$) from our linear-stability analysis. Both panels indicate a minimum radius for oscillations of $R_{\min} = 0.45\ \mu$m.

Conclusion and outlook

Min-protein oscillations in rod-shaped *E. coli* cells block cell division at the poles, thereby preventing minicelling. The Min system may also contribute to the accuracy of cell division. Wild-type *E. coli* forms an FtsZ ring at the cell center with an accuracy better than $\pm 1\%$ of cell length, and this accuracy is lost in *min*$^-$ mutants [11]. An alternative view is that this loss of accuracy may simply reflect the onset of minicelling, rather than indicating a direct role for the Min system in division accuracy [23]. (Indeed in *Bacillus subtilis*, homologs of MinC and MinD statically localize to the poles to prevent minicelling and have been shown to be dispensable for division accuracy [24].) Division-site placement in *E. coli* is regulated both by the Min-protein system and by nucleoid occlusion [10]. Certainly, in rod-shaped cells, Min oscillations and division accuracy, possibly based on nucleoid occlusion, could be independent, with both relying on the obvious long axis of the cell.

In round cells (cocci) such as *N. gonorrhoeae* there is no obvious long axis. Nevertheless, cocci divide accurately along an equatorial plane into two daughter cells. If the Min proteins oscillate in *N. gonorrhoeae*, as experiments [13, 14] and our numerical results suggest, then for the Min system to perform its usual function of blocking polar divisions requires that the poles and equator of the cell be

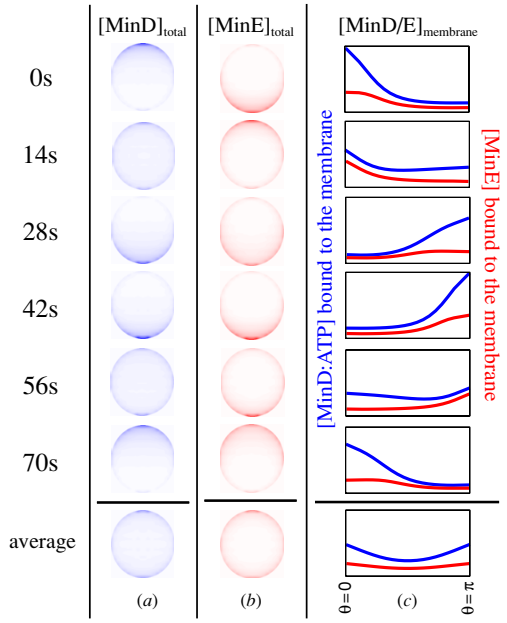

Figure 4. Time slices in 14 s increments of one complete MinD,E oscillation in an ellipsoidal cell with semi-major axis of length $R_1 = 0.525\ \mu$m and semi-minor axes of length $R_2 = 0.5\ \mu$m. The quantities shown in (*a*), (*b*) and (*c*) are the same as in figure 2. Starting from a random initial distribution of proteins, pole-to-pole oscillations along the long axis become established within 3 oscillation periods. The y-axis on each plot in (*c*) ranges from 0 to 600 μm^{-2}.

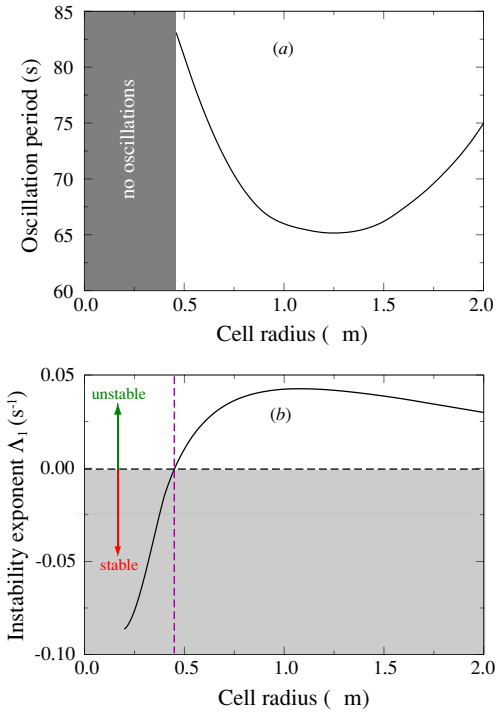

Figure 5. (*a*) Oscillation period as a function of cell radius. For cells with a radius smaller than $R_{\rm min} = 0.45\ \mu$m, no oscillations are possible. (*b*) Instability exponent Λ_1 as a function of cell radius for the most unstable perturbation ($\sim \cos\theta$) superimposed on a static, spherically symmetric solution.

consistently defined. This point is made in the schematic in figure 6, with the schematic nucleoid segregation representing the full machinery of accurate cell division. The requirement for consistency between poles (MinCD accumulation zones) and equator (division plane) suggests that Min oscillations and division accuracy are directly coupled in *N. gonorrhoeae*. Experiments in round *E. coli* mutants [15] indicate that Min oscillations can pick out the long axis in slightly asymmetric cells. Our numerical simulations in ellipsoidal cells support this conclusion, and it is tempting to speculate that for cell division in *N. gonorrhoeae*, the Min oscillations exploit small variations in cell shape to define the poles and equator of the cell.

The ability of the Min oscillations to select the long axis of an ellipsoidal cell reflects the length dependence of the oscillatory instability. As shown in figure 5(*b*), the instability exponent Λ_1 increases with radius. Therefore, in asymmetric cells the oscillation pattern with the longest wavelength will become established. In the case of an ellipsoidal cell, the longest wavelength pattern corresponds to oscillations along the long axis of the cell. In both ellipsoidal and rod-shaped cells, a protein oscillator which prefers long wavelengths can provide a general mechanism for polar targeting of proteins.

In the most spherical of their round *rodA*$^-$ *E. coli* cells, Corbin *et al* [15] observed rapid reorientation of Min oscillations of the MinD$_{\rm Ng}$ proteins. Ramirez-Arcos *et al* [14] also observed uncoordinated oscillations in large

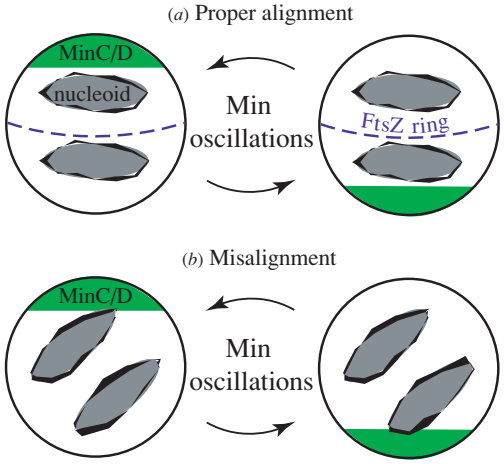

Figure 6. Schematic of pre-division round cell. (*a*) The alignment of the Min oscillations and nucleoid segregation ensures proper formation of the FtsZ ring. (*b*) Misalignment of the axial direction of the Min oscillations and the equator defined by the segregated nucleoids prohibits FtsZ-ring formation.

rodA$^-$ *E. coli* cells, but saw consistent pole-to-pole oscillations in smaller *rodA*$^-$ cells. In so far as the Min oscillations have a preferred wavelength for oscillations [17], it is

not surprising that qualitatively different oscillation patterns were observed in differently-sized round cells. Indeed, our numerical results suggest that the mislocalized oscillation patterns observed in large round cells reflect the instability of higher-order oscillation modes. Specifically, we found that larger cells, with radii $R > 0.7$ μm, starting from a north–south-symmetric protein distribution, support an oscillatory solution where the MinD distribution alternates between simultaneous accumulations at both poles and an equatorial accumulation. Moreover, in our simulations of cells with radii larger than $\sim$1.2 μm, we observe oscillations in which the MinD accumulates at intermediate locations between the pole and equator rather than at the pole. These patterns, which can be understood as a combination of pole-to-pole oscillations with higher-order oscillation modes, would be sensitive to fluctuations and nucleation effects in real cells. Indeed, the specific movement of the MinD 'pole' in large *rodA*$^-$ *E. coli* cells is likely a consequence of nucleation effects, i.e., in the regime of cell sizes where accumulation can occur near the equator, the first significant accumulation of MinD away from the old pole becomes the new pole. This nucleation effect is beyond the scope of our current mean-field model for Min oscillations. Even for rod-shaped cells, it remains an open question how fluctuations affect the stability and character of Min oscillations. The recent observation by Shih *et al* [6] that MinD accumulates in helical polymers which remain present even at the 'empty' pole may help explain why fluctuations do not lead to uncoordinated oscillations in wild-type cells.

The role of Min oscillations in nucleoid segregation and cell-division accuracy remains an important open question. We are currently focused on imaging Min proteins in *N. gonorrhoeae* to verify that the Min system forms a spatial oscillator. Two-color fluorescence microscopy experiments, labeling MinD and FtsZ, will test whether the Min oscillations properly align with the division plane to achieve accurate nucleoid segregation. The correlation of the oscillation axis with the cell shape will demonstrate whether elongation of the cell orients the Min oscillations.

Acknowledgments

The authors would like to thank Bonnie Bassler, Joe Lutkenhaus, William Margolin, Yigal Meir and Tom Silhavy for valuable suggestions and readings of the manuscript. Partial funding for this research was provided by the MRSEC program of the NSF under grant number DMR-0213282.

Glossary

GFP-fusion. Translational fusion to Green Fluorescent Protein (GFP) used to tag a specific protein for visualization with subcellular fluorescence microscopy.

Linear-stability analysis. Method of determining whether the steady-state solution of a system of equations (e.g. reaction-diffusion equations) is stable with respect to a given perturbation.

Ellipsoid. A distorted sphere which has been elongated in one direction. The surface of an ellipsoid with major axis along the z-axis satisfies the equation

$$\left(\frac{x}{R_{\text{minor}}}\right)^2 + \left(\frac{y}{R_{\text{minor}}}\right)^2 + \left(\frac{z}{R_{\text{minor}}}\right)^2 = 1.$$

Protein targeting. The direction of proteins to particular cellular regions, e.g. the cell poles.

Nucleoid segregation. Separation of the nucleoids to opposite halves of the cell prior to cell division to allow for septum formation.

Cell-division accuracy. How accurately the cell divides into two equal daughter cells, i.e. how close cell division is to midcell. In units of cell length, wild-type *E. coli* divides with accuracy 0.50 ± 0.01 [11].

References

[1] de Boer P A J, Crossley R E and Rothfield L I 1989 A division inhibitor and a topological specificity factor coded for by the Minicell Locus determine proper placement of the division septum in *E. coli Cell* **56** 641
[2] Raskin D M and de Boer P A J 1999 Rapid pole-to-pole oscillation of a protein required for directing division to the middle of *Escherichia coli Proc. Natl Acad. Sci. USA* **96** 4971
[3] Hu Z and Lutkenhaus J 1999 Topological regulation of cell division in *Escherichia coli* involves rapid pole to pole oscillation of the division inhibitor MinC under the control of MinD and MinE *Mol. Microbiol.* **34** 82
[4] Fu X, Shih Y-L, Zhang Y and Rothfield L I 2001 The MinE ring required for proper placement of the division site is a mobile structure that changes its cellular location during the *Escherichia coli* division cycle *Proc. Natl Acad. Sci. USA* **98** 980
[5] Huang J, Cao C and Lutkenhaus J 1996 Interaction between FtsZ and Inhibitors of Cell Division *J. Bacteriol.* **178** 5080
[6] Shih Y-L, Le T and Rothfield L 2003 Division site selection in *Escherichia coli* involves dynamic redistribution of Min proteins within coiled structures that extend between the two cell poles *Proc. Natl Acad. Sci. USA* **100** 7865
[7] Hu Z, Gogol E P and Lutkenhaus J 2002 Dynamic assembly of MinD on phospholipid vesicles regulated by ATP and MinE *Proc. Natl Acad. Sci. USA* **99** 6761
[8] Bi E and Lutkenhaus J 1993 Cell division inhibitors SulA and MinCD prevent formation of the FtsZ ring *J. Bacteriol.* **175** 1118
[9] Bi E and Lutkenhaus J 1991 FtsZ ring structure associated with division in *Escherichia coli Nature* **354** 161
[10] Woldringh C L, Mulder E, Valkenburg J A, Wientjes F B, Zaritsky A and Nanninga N 1990 Role of the nucleoid in the toporegulation of division *Res. Microbiol.* **141** 39
[11] Yu X-C and Margolin W 1999 FtsZ ring clusters in *min* and partition mutants: role of both the Min System and the nucleoid in regulating FtsZ ring localization *Mol. Microbiol.* **32** 315
[12] Wu L J and Errington J 2004 Coordination of cell division and chromosome segregation by a nucleoid occlusion protein in *Bacillus subtilis Cell* **117** 915
[13] Szeto J, Ramirez-Arcos S, Raymond C, Hicks L D, Kay C M and Dillon J-A R 2001 Gonococcal MinD affects cell division in *Neisseria gonorrhoeae* and *escherichia coli* and exhibits a novel self-interaction *J. Bacteriol.* **183** 6253

[14] Ramirez-Arcos S, Szeto J, Dillon J-A R and Margolin W 2002 Conservation of dynamic localization among MinD and MinE orthologues: oscillation of *Neisseria gonorrhoeae* proteins in *Escherichia coli Mol. Microbiol.* **46** 493
[15] Corbin B D, Yu X-C and Margolin W 2002 Exploring intracellular space: function of the Min system in round-shaped *Escherichia coli EMBO J.* **21** 1998
[16] Pichoff S, Vollrath B, Touriol C and Bouché J-P 1995 Deletion analysis of gene *minE* which encodes the topological specificity factor of cell division in *Escherichia coli Mol. Microbiol.* **18** 321
[17] Huang K C, Meir Y and Wingreen N 2003 Dynamic structures in *Escherichia coli*: Spontaneous formation of MinE rings and MinD polar zones *Proc. Natl Acad. Sci. USA* **100** 12724
[18] Howard M, Rutenberg A D and de Vet S 2001 Dynamic compartmentalization of bacteria: accurate division in *E. coli Phys. Rev. Lett.* **87** 278102
[19] Meinhardt H and de Boer P A J 2001 Pattern formation in *Escherichia coli*: a model for the pole-to-pole oscillations of Min proteins and the localization of the division site *Proc. Natl Acad. Sci. USA* **98** 14202
[20] Kruse K 2002 A dynamic model for determining the middle of *Escherichia coli Biophys. J.* **82** 618
[21] Shih Y-L, Fu X, King G F, Le T and Rothfield L 2002 Division site placement in *E. coli*: mutations that prevent formation of the MinE ring lead to loss of the normal midcell arrest of growth of polar MinD membrane domains *EMBO J.* **21** 3347
[22] Elowitz M B, Surette M G, Wolf P-E, Stock J B and Leibler S 1998 Protein mobility in the cytoplasm of *Escherichia coli J. Bacteriol.* **181** 197
[23] Margolin W 2004 Private communication
[24] Migocki M D, Freeman M K, Wake R G and Harry E J 2002 The Min system is not required for precise placement of the midcell Z ring in *Bacillus subtilis EMBO Rep.* **3** 1163